



Synthetic fluorescent probes for studying copper in biological systems

Journal:	<i>Chemical Society Reviews</i>
Manuscript ID:	CS-REV-10-2014-000346.R1
Article Type:	Review Article
Date Submitted by the Author:	18-Oct-2014
Complete List of Authors:	Chang, Chris; University of California, Berkeley, Department of Chemistry Cotruvo, Jr., Joseph; University of California, Berkeley, Department of Chemistry Aron, Allegra; University of California, Berkeley, Department of Chemistry Ramos-Torres, Karla; University of California, Berkeley, Department of Chemistry

Chemical Society Reviews: Special Issue on Sensing and Imaging

Synthetic fluorescent probes for studying copper in biological systems

Joseph A. Cotruvo, Jr.,^a Allegra T. Aron,^a Karla M. Ramos-Torres,^a and Christopher J. Chang^{*,a,b,c}

^a *Department of Chemistry, University of California, Berkeley, CA 94720, USA*

^b *Department of Molecular and Cell Biology, University of California, Berkeley, CA 94720, USA*

^c *Howard Hughes Medical Institute, University of California, Berkeley, CA 94720, USA*

** Corresponding author: chrischang@berkeley.edu; Fax: +1 510 642-7301; Tel: +1 510 642-4704*

Synopsis: This review surveys fluorescent probes for copper, emphasizing desirable criteria for their effective use for discovery and study of new metal biology.

Abstract: The potent redox activity of copper is required for sustaining life. Mismanagement of its cellular pools, however, can result in oxidative stress and damage connected to aging, neurodegenerative diseases, and metabolic disorders. Therefore, copper homeostasis is tightly regulated by cells and tissues. Whereas copper and other transition metal ions are commonly thought of as static cofactors buried within protein active sites, emerging data points to the presence of additional loosely bound, labile pools that can participate in dynamic signalling pathways. Against this backdrop, we review advances in sensing labile copper pools and understanding their functions using synthetic fluorescent indicators. Following brief introductions to cellular copper homeostasis and considerations in sensor design, we survey available fluorescent copper probes and evaluate their properties in the context of their utility as effective biological screening tools. We emphasize the need for combined chemical and biological evaluation of these reagents, as well as the value of complementing probe data with other techniques for characterizing the different pools of metal ions in biological systems. This holistic approach will maximize the exciting opportunities for these and related chemical technologies in the study and discovery of novel biology of metals.

1. Introduction

Copper is an essential element for life,¹ particularly after the advent of oxygenic photosynthesis, which facilitated oxidation of the relatively insoluble Cu(I) to the more water-soluble Cu(II) and increased its availability for biological utilization.² The cellular biochemistry of copper in eukaryotes is diverse and far-ranging, as this metal serves as an essential cofactor for numerous redox enzymes that react with dioxygen and its reduced derivatives like superoxide ($O_2^{\cdot-}$).^{3,4} These enzymes are involved in critical processes such as respiration [e.g., cytochrome *c* oxidase (CcO)],⁵⁻⁷ electron transfer/substrate oxidation and iron uptake (ceruloplasmin),⁸ pigmentation (tyrosinase),⁹ antioxidant defence (Cu/Zn superoxide dismutases),¹⁰⁻¹⁴ neurotransmitter synthesis and metabolism (dopamine β -hydroxylase, peptidylglycine α -amidating monooxygenase),¹⁵⁻¹⁸ epigenetic modification (lysyl oxidase-like 2),¹⁵ and handling of dietary amines (copper amine oxidases).^{16,17} On the other hand, misregulation of copper is also implicated in human genetic disorders like Menkes¹⁸⁻²⁰ and Wilson's²¹⁻²³ diseases; neurodegenerative diseases²⁴ such as Alzheimer's,²⁵⁻²⁸ Parkinson's,²⁹ prion,^{30,31} and Huntington's³² diseases and familial amyotrophic lateral sclerosis;³³ and metabolic disorders such as obesity and diabetes.³⁴⁻³⁸ More recently, copper has also been found to regulate cancers that operate through widely observed oncogenic BRAF mutations^{6,39,40} and influence tumour growth. In addition to the canonical, tightly bound pool of copper, the observation of a reversibly and relatively loosely bound ("labile") pool of copper in cells,⁴¹⁻⁴⁴ likely buffered by low molecular weight ligands like glutathione (GSH), is particularly intriguing, presaging that copper and related transition metals in these more bioavailable forms can also participate in dynamic cell signalling pathways.

In many of the aforementioned examples, the very same redox activity that makes copper a potent physiological element can also be deleterious to the cell via aberrant chemistry of reactive oxygen and nitrogen species.^{45,46} Consequently, the delicate balancing act between the physiological and pathological roles of copper has led to significant interest in how it is properly and improperly handled in the cell. This central question motivates the development of new technologies that enable monitoring total metal content in biological specimens and the partitioning of metal ions into static, enzyme-bound and dynamic, labile pools with cellular and subcellular resolution. Traditional bulk techniques such as atomic absorption spectroscopy and inductively coupled plasma mass spectrometry (ICP-MS),⁴⁷ along with use of radioactive isotopes (e.g., ⁶⁴Cu),^{48,49} provide direct information on total metal content. As the metal content of a single cell (10^{-15} g)⁵⁰ is too low for bulk measurements, however, several synchrotron-based⁵¹ methods for elemental analysis of single cells with greater sensitivity and with spatial resolution have emerged in recent years. X-ray fluorescence microscopy (XFM)⁵² visualizes the elemental distribution of a chemically or cryofixed sample by detection of the characteristic fluorescence emission signatures from the constituent atoms with sensitivity of 10^{-18} g, and it has been recently applied to copper biology.^{41,44,53-56} Micro X-ray absorption near edge structure (micro-XANES) offers information on the oxidation state and coordination environment of the metal ion.^{44,57} Nano-secondary ion mass spectrometry (Nano-SIMS, a mass-spectrometry imaging technique capable of measuring secondary ions ejected from a solid sample) has similar capabilities to XFM but detects mass rather than fluorescence.⁵⁷ Laser ablation (LA) ICP-MS⁵⁸ offers an alternative to XFM and Nano-SIMS that is less sensitive but uses less sophisticated instrumentation.

An emerging set of complementary chemical reagents to sense the labile copper pools derived from the total metal pool is molecular imaging using copper-responsive fluorescent

probes. This method enables real-time detection of the copper ion analyte in live cells and more complex specimens. Because these probes are ideally in equilibrium with endogenous ligands while minimally perturbing cellular pathways, they cannot report on the absolute copper ion concentration but rather provide relative information on the availability and distribution of labile copper pools in cells. However, because this approach relies on the chemical behaviour of the analyte and reporter, rather than intrinsic physical properties, it comes with the challenges of sensitive and selective detection in the complex, heterogeneous environment of the cell. This complexity, in turn, requires the application of multiple independent analytical methods and controls, both chemical and genetic, to validate their proper use in each and every different biological context. This review summarizes advances in synthetic fluorescent sensors for Cu(I), the predominant oxidation state of copper in the cellular reducing environment, emphasizing the design and validation of reagents that enable biological study. We conclude with a discussion to highlight new opportunities and guide the development of improved technologies for exploring and identifying the diverse roles of copper and other transition metals in biological systems.

2. Overview of biological copper homeostasis

To provide a backdrop for biological application of fluorescent probes for Cu(I), we present an overview of copper homeostasis, together with a discussion of biological copper coordination chemistry. We refer the reader to several excellent reviews for more comprehensive treatments of copper homeostasis.^{4,59-61} Here, we briefly outline the basic principles underlying the handling of copper in biology, as well as introduce the major protein and small-molecule players relevant to detection of the availability and distribution of labile copper.

The two major oxidation states of copper in living systems are Cu(I) and Cu(II), the former being more kinetically labile and favoured within the reducing environment of the cell. Specificity for delivering Cu(I) to the right place at the right time in the right amount is achieved by two main mechanisms, (1) subcellular compartmentalization and (2) use of metallochaperone proteins. In the first strategy, the cell maintains distinct metal concentrations in different cellular compartments. For example, prokaryotes generally restrict copper proteins to the periplasm to avoid copper outcompeting other metals in the cytosol; in one elegant example by Robinson and co-workers, folding of a metalloprotein in the cytosol versus in the periplasm controls whether it is metallated with manganese or copper.⁶² Alternatively, in the case of metal overload, the metal can be sequestered in a special compartment to protect against mismetallation rather than be exported from the cell;⁶³ recent work by Merchant and colleagues demonstrates sequestration of copper in lysosome-like structures within zinc-deficient algae.⁵⁷ In the second strategy, the cell has evolved proteins called metallochaperones to selectively bind and escort a specific metal ion through the cell, with selectivity of metal ion transfer determined by protein-protein interactions.⁶⁰ Whereas absolute values vary depending on methods of analysis and can also vary by environmental factors such as ionic strength and additives that influence parameters like hydrophobicity, etc,⁶⁴⁻⁶⁶ the relative values of the apparent dissociation constants of proteins and small molecules known to be involved in copper trafficking pathways (Table 1) suggest that copper follows an affinity gradient from relatively low-affinity ligation at its point of uptake, higher affinity for the metallochaperones, and highest affinity at its ultimate destination. Thus the cell helps to ensure that, in the presence of several other metal ions and myriad potential metal-binding proteins in the complex cytosolic environment, copper is efficiently directed to its intended targets when needed in tightly bound protein forms. Notably, metallochaperone-

mediated metal transfer has been found to be associative, suggesting a kinetically labile copper pool in the multi-component buffering system of the cell.

In some cases, metal transfer is also driven by an irreversible step at the target protein following copper loading, such as a conformational change⁶⁷ or oxidation of Cu(I) to Cu(II).⁶⁸ Even in these pathways, the presence of many reversible upstream steps enables the possibility of cell signalling being mediated by copper in early steps between relatively low-affinity binding partners. For example, the single most abundant thiol in the eukaryotic cell is glutathione (GSH), present at 1-10 mM concentrations.⁶⁹ GSH forms a variety of complexes with Cu(I), but the complex with 1:1 Cu(I):GSH stoichiometry that is the primary species identified *in vitro*⁷⁰ has a reported apparent K_d of 9×10^{-12} M (Table 1). This value is relatively weak compared to Cu(I) chaperone proteins, but the cellular abundance of GSH likely offsets this low affinity. Many dynamic copper sites that can exchange with GSH or other small-molecule ligands, or form ternary species via partial ligand exchange, remain to be discovered.

Table 1. Apparent dissociation constants for Cu(I)-binding proteins and small-molecule ligands

Protein/Ligand	K_d (fM) ^a
Atox1	16.8
ATP7A (Menkes)	
MBD1 ^b	2.5
MBD2	4.9
MBD3	104
MBD5	13.0
MBD6	2.6
CCS ^c	2.4
SOD1 Cu site	0.23
MT-2 ^d	0.41
GSH	9130
Dithiothreitol (DTT)	7940 ^e

^a Ref. ⁶⁴

^b MBD: metal binding domain

^c CCS: copper chaperone for Cu,Zn superoxide dismutase (SOD1)

^d MT-2: Metallothionein 2

^e Ref. ⁷¹

The major players in copper homeostasis within a generic eukaryotic cell are shown in Figure 1. Extracellular Cu(II) is reduced to Cu(I) by an unknown mechanism and intracellular accumulation occurs mainly through the high-affinity Cu(I) channel copper transporter 1 (CTR1). (A low-affinity copper transport system also exists, although its identity has not yet been established.⁴⁸) CTR1 is a trimeric, plasma membrane-spanning copper ion channel, containing an N-terminal, Met- and His-rich domain and a transmembrane MX₃M motif important for Cu(I) uptake.⁷²⁻⁷⁴ Use of these ligands for Cu(I) provides a manner of resistance to the relatively oxidizing extracellular environment.⁷⁵ An analogue of CTR1, CTR2, is involved in copper release from endosomes.⁷⁶ Once inside the cell, copper ions are delivered to various destinations with the cytosol and other organelles by a suite of metallochaperones, including

Atox1, CCS, and Cox17. This situation does not rule out the formation of ternary complexes between GSH, CTR1 and metallochaperones as competent intermediates owing to the high intracellular concentration of GSH. CCS is the copper metallochaperone for SOD1, and Cox17 regulates mitochondrial copper delivery. Atox1 delivers Cu(I) via an associative mechanism to ATP7A and ATP7B,⁷⁷ which then go on to metallate proteins in the secretory pathway and/or control copper efflux from the cell.⁷⁸ Under basal levels of copper, ATP7A/B primarily reside in the trans-Golgi network, where they transport Cu(I) in an ATP-dependent manner from the cytoplasm into the secretory pathway for metallation of proteins such as ceruloplasmin (the major copper carrier in the blood), tyrosinase, and lysyl oxidase. Increased copper levels lead to the trafficking of ATP7A/B toward the cell surface, which represents the major pathway for copper efflux. More recent work has also implicated ATP7B in copper delivery to lysosomal compartments in a copper-dependent manner.⁷⁹ Metallothioneins (MTs) are an additional Cys-rich set of proteins that are implicated in resistance to high concentrations of Cu(I), Zn(II), and Cd(II), resistance to oxidative stress, and copper and zinc trafficking.⁸⁰ Finally, the list of proteins involved in mitochondrial copper homeostasis is rapidly expanding,⁸¹⁻⁸³ and beyond these protein pools, there is also evidence for a small-molecule copper-binding ligand of unknown structure, CuL.^{84,85} This species, which can be purified in its copper-complexed form, can represent up to ca. 60% of total mitochondrial copper present in the matrix.⁸²

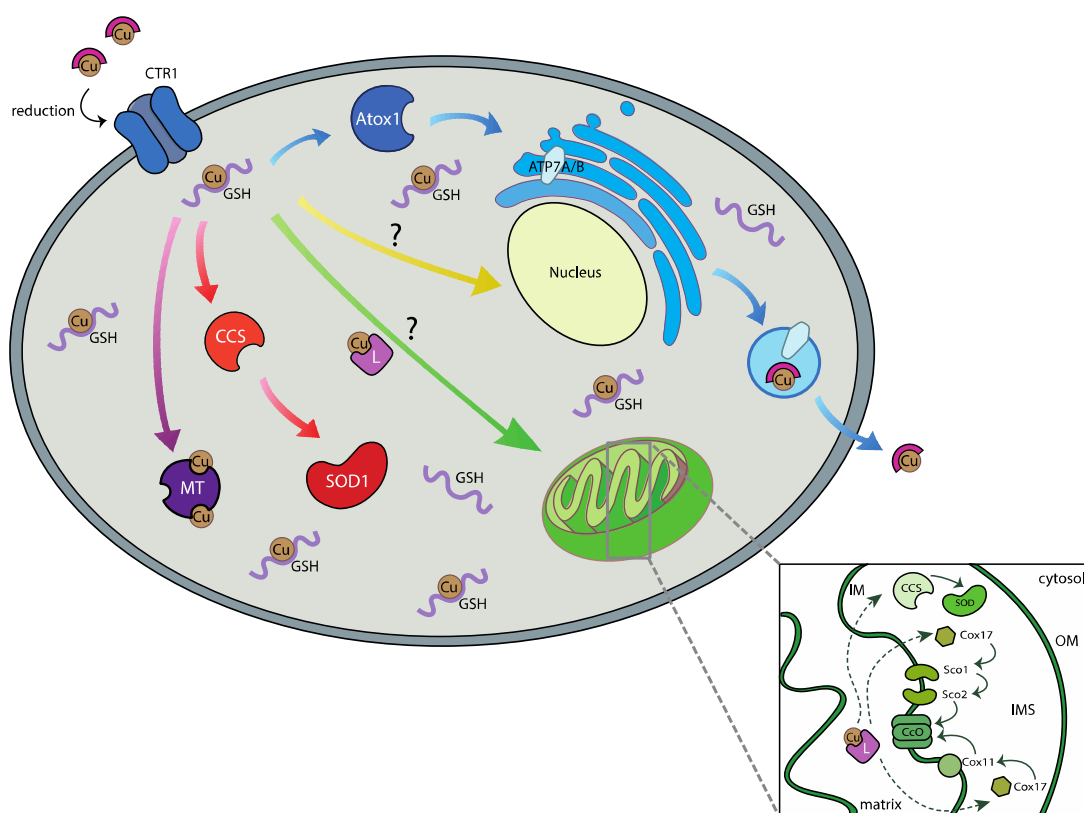


Figure 1. A simplified overview of copper handling pathways in a generic eukaryotic cell. Cu(II) is reduced to Cu(I) by an unknown mechanism and can enter the cell through CTR1, the principal high-affinity copper importer. Upon entry, copper interacts with cellular ligands and with chaperones that mediate its delivery to specific proteins. Glutathione (GSH) can buffer Cu(I) pools and mediate Cu(I) transfer between CTR1 and metallochaperones.⁸⁶ Atox1 is the metallochaperone responsible for copper delivery to two ATPases, ATP7A and ATP7B, in the trans-Golgi network, where most cuproproteins are metallated, and are also involved in copper efflux from the cell. Delivery of copper to cytosolic SOD1 proceeds through the metallochaperone CCS. In the mitochondrion, an ensemble of mitochondrial proteins is required for metallation of the cytochrome *c* oxidase (CcO) complex. Cox17 delivers copper to Cox11 for the Cu_B site of CcO, while also delivering copper to Sco1 and Sco2 for the Cu_A site. CCS present in the intermembrane space (IMS) provides copper to a mitochondrial pool of SOD1. The small copper ligand (L) is proposed to buffer copper in the mitochondrion and may also be involved in copper delivery to that organelle. Metallothioneins (MTs) bind Cu tightly and protect the cell against copper overload and oxidative stress. Whereas XFM data show the presence of copper in the nucleus, its mechanism of transport and its nuclear ligands are currently unknown.

Although continually evolving, our current understanding of copper homeostasis can be summarized with four basic points: (1) subcellular compartmentalization provides a versatile mechanism for controlling available ligands for copper, and by extension, other metal pools, (2) a wide range of relative binding affinities for copper ligands exist in the cell as a multi-component buffer, (3) copper trafficking is reversibly driven by affinity gradients from relatively weak ligands (e.g. CTR1 and GSH) to tighter binding target proteins (e.g. SOD1) via metallochaperones (e.g. Atox1, CCS, Cox17), and (4) copper trafficking is dominated by surface sites with low coordination number with transfer occurring by specific interactions and an associative mechanism. These last two principles indicate that there exists a thermodynamically labile pool of Cu(I) and suggest that this pool may also be kinetically labile, noting that labile is not to be equated with free or aquated metal. There are few characterized roles for these pools of copper^{39,40} (as well as of other transition metal ions)⁸⁷ at present, but it is likely that they modulate enzyme activity and protein function through reversible binding and reaction with small molecules.⁸⁸ In this context, fluorescent probes for Cu(I) are best employed as qualitative screening tools to monitor the availability and dynamic distributions of this labile pool—a subset of the total copper pool, which can be directly and quantitatively measured using bulk techniques (e.g., ICP methods, XFM, and NanoSIMS)—to set the stage for more detailed biological inquiries.

3. Design principles for developing Cu(I) sensors of biological utility

The development of effective chemical reagents to probe copper biology requires meeting a host of strict chemical and biological criteria,⁸⁹ as performing chemistry or biology in isolation from the other can afford insufficient data to draw meaningful conclusions. Important chemical properties include high selectivity for Cu(I) with metal and oxidation state specificity over competitors in the biological milieu – in particular, cellularly abundant Na(I), K(I), Mg(II), and Ca(II), as well as Zn(II), Cu(II), and Fe(II)/Fe(III) as major d-block competitors. In terms of photophysical properties, a fast, high signal-to-noise response with an increase or ratiometric excitation/emission wavelength shift is preferred over turn-off probes in order to maximize spatial resolution as well as high optical brightness to allow for minimal dye loading in imaging applications. In this context, Cu(I) and other d-block metals are well-known to quench

fluorescence of dyes,⁹⁰ making the development of turn-on probes challenging for the transition metal series, compared to widely employed Ca(II) and Zn(II) indicators.⁹¹⁻⁹⁴

For use in cellular imaging, visible wavelength excitation/emission is ideal, as inner-filter interference and autofluorescence from native cellular components like NAD(P)H, flavins, and haem can complicate interpretation of data obtained with UV-excitable probes. Two-photon microscopy may circumvent some of these issues but remains less available compared to one-photon instrument systems. Photostability is important for live imaging applications, meaning that the most useful probes must be resistant to photobleaching over the entire experimental timescale at relevant laser powers. Because a metal-responsive probe is involved in dynamic equilibrium with competing small-molecule and protein ligands in the cell, effective reagents must be matched with the appropriate apparent K_d values for a given cell type and stimulation. Notably, complete ligand exchange may not be necessary to obtain a useful turn-on or wavelength-shift ratiometric response to copper, as in the case of broadly-used Zn(II) fluorophores TSQ⁹⁵ and Zinquin⁹⁶ for qualitative labile Zn(II) screening assays. The heterogeneity and diversity of biological systems makes relative, not absolute, fluorescence responses most useful for comparison. Finally, biocompatibility is also necessary, meaning that effective probes must retain the ability to reversibly sense increases or decreases in labile Cu(I) in the presence of lipids, proteins, sugars, and metal-interacting small-molecules such as GSH in a given biological context.

As virtually any organic fluorescent dye will have extended conjugation and thus be relatively hydrophobic, the absolute responses in pure aqueous buffer and buffer with various model organic components will certainly vary, but the relative response to added copper, chelator, or genetic manipulation compared to background still gives valuable information. Fluorescent reagents typically are designed and physically characterized by chemists in tightly controlled *in vitro* environments, but biologists may use them in vastly divergent cells, tissues, and animal systems where solubility, intracellular distribution and reactivities are more heterogeneous. For this reason, it is important to aim to rigorously test each probe in its intended application, as there is no one-size-fits all chemical reagent, probe or chelator, for every biological assay. No *in vitro* assay can perfectly, faithfully mimic a cellular environment and such chemical data should not be over-interpreted when performed in isolation without supporting biological controls. Moreover, metal supplementation and chelation experiments, accompanying complementary methods for direct bulk analysis of metal accumulation and depletion (e.g., ICP, XFM, and Nano-SIMS), along with genetic controls for copper depletion and/or hyperaccumulation, can show the reversibility and robustness of a given chemical probe in a given biological context.

4. Overview of advances in the development of Cu(I) fluorescent indicators

With these principles in mind, we now survey advances in the development of fluorescent probes toward the study of biological Cu(I). Most of the available turn-on fluorescent sensors for Cu(I) are based on a fluorescence switching mechanism dependent on a photoinduced electron transfer (PET) process or a related charge transfer (CT) pathway, as detailed in papers originating from the classic Ca(II) indicators of Tsien⁹⁷ and further elucidated by de Silva,^{98,99} Czarnik,¹⁰⁰ Nagano,^{101,102,103} and others. In the “off-state,” excitation of the fluorophore produces a charge-separated state through an electron transfer from the receptor to the excited-state fluorophore, thereby quenching fluorescence. When analyte Cu(I) is bound to the electron-rich receptor, the PET process is inhibited, enabling a fluorescence “on-state”. For this PET-

dependent quenching to be thermodynamically favourable, to an approximation, the reduction potential of the excited-state fluorophore (acceptor) must be more positive than that of the receptor (donor).^{104,105} Coordination to the cationic analyte produces an electrostatic attraction between the analyte and an electron in the highest occupied molecular orbital (HOMO) of the receptor, decreasing the oxidation potential (increasing the reduction potential) of the analyte-bound receptor sufficiently to render the thermodynamics of PET no longer favourable (Figure 2).^{98,106} This fluorescence switching mechanism offers an opportunity to finely tune the thermodynamic and photophysical properties of fluorescent probes by synthetically altering the reduction and oxidation potentials of its components and the excited-state equilibrium energy, as shown in previous studies^{103,107-109} and can be inverted into a donor PET mechanism as well.¹¹⁰ Chemical structures of various Cu(I) probes are depicted in Figure 3 and key properties are shown in Table 2.

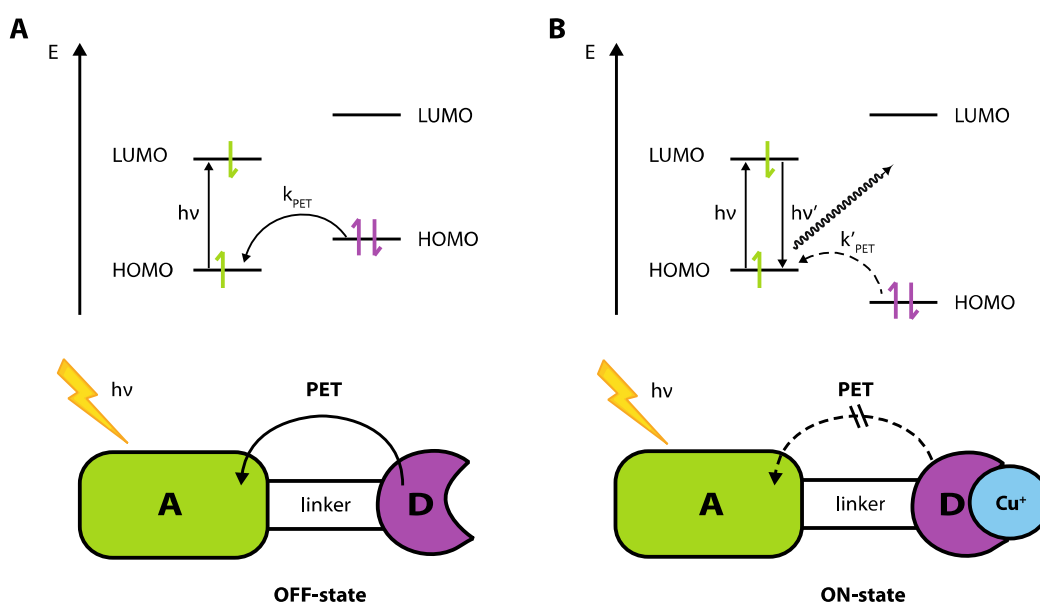


Figure 2. Energy level diagram from the frontier molecular orbital perspective illustrating the fluorescence switching of Cu(I)-fluorescent indicators based on a photoinduced electron transfer (PET) mechanism. (A) In the absence of Cu(I), electron transfer from the electron-rich donor (D) to the photoexcited fluorophore acceptor (A) is favourable resulting in fluorescence quenching. (B) Complex formation with Cu(I) lowers the donor HOMO energy, slows down the rate of electron transfer (k'_{PET}), and restores fluorescence.

Table 2. Photophysical and thermodynamic properties of selected fluorescent probes for Cu(I)

Sensor	Absorption λ_{max} (nm)	Emission λ_{max} (nm)	Φ^a	f_e^b	K_d (M)	Reference
CTAP-1	365	485	0.14	4.6	4×10^{-11}	44
CTAP-2	396	508	0.083	65	4×10^{-12}	111
CS1	540	561	0.13 (67) ^e	10	4×10^{-12}	112
CS3	540	548	0.40	75	9×10^{-14}	41
Mito-CS1	550	558	0.05	10	7×10^{-12}	113

ACu1	365 (750) ^c	482	0.13	4	2×10^{-11}	114
CS790	760	790	0.072	15	3×10^{-11}	115
Probe 3	750	792	n.d. ^d	9.6	6×10^{-12}	116
FluTPA1	470	513	0.37	1500 ^f	n.d. ^d	117
CR3	529	545	0.15	13	1×10^{-13}	43
CF3	534 (910) ^c	557	0.22	40	3×10^{-13}	43

^a Fluorescence quantum yield

^b Fluorescence turn-on in vitro [maximum ratio of fluorescence intensity upon Cu(I) binding to intensity of apo sensor]

^c Value in parenthesis is for two photon absorption

^d N.D.: not determined

^e Value in parenthesis is two photon absorption cross section ($\Phi\beta$) in GM, at indicated two photon absorption

^f After 2 h incubation under reported conditions

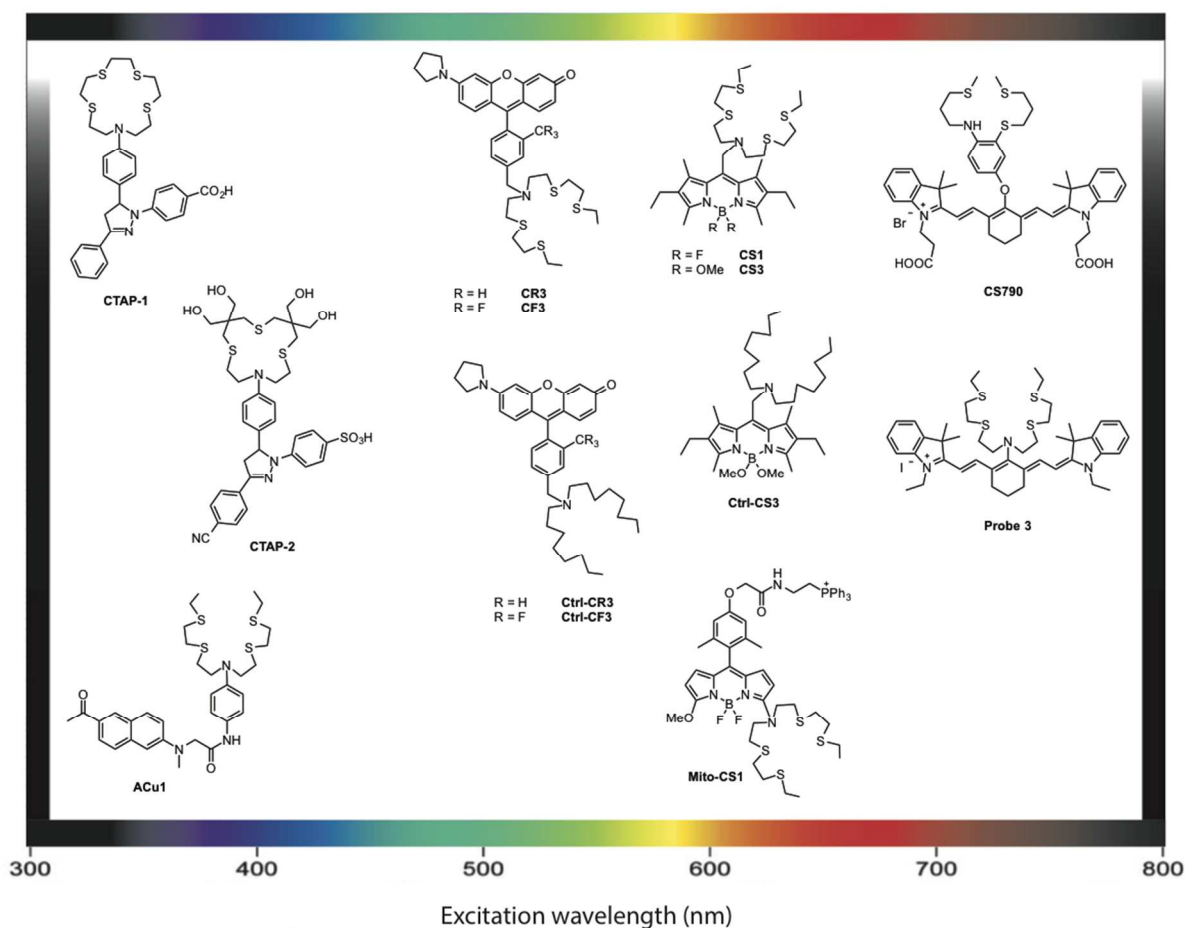


Figure 3. Chemical structures of fluorescent probes for Cu(I) detection.

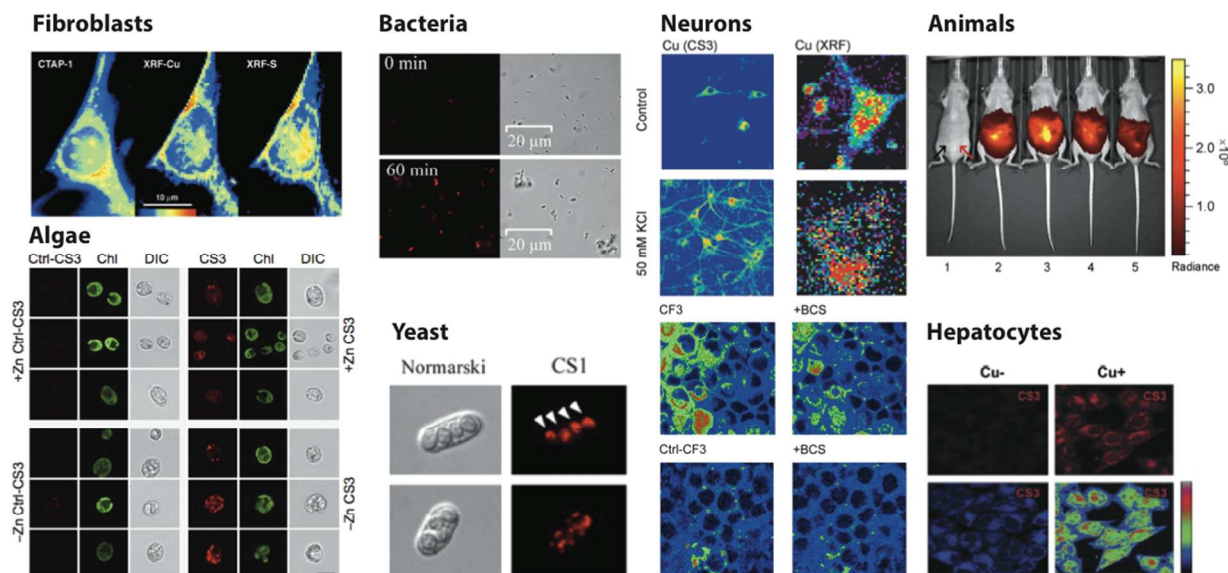


Figure 4. Biological studies making use of fluorescent probes for Cu(I) detection in various models, including fibroblasts,⁴⁸ bacteria,¹²⁶ neurons,^{45,47} animals,¹¹⁹ algae,⁶¹ yeast,¹²⁹ and hepatocytes.⁸³

4.1. Pyrazoline-based copper probes

Fahrni and co-workers reported CTAP-1 (Figure 3, Table 2), the first small-molecule fluorescent sensor for Cu(I),⁴⁴ comprised of a 1,3-diarylpyrazoline fluorophore linked to a tetrathiazacrown ether receptor (NS₄). CTAP-1 features high selectivity for Cu(I) with a ca. 5-fold turn-on response upon UV excitation at 365 nm. This important early work demonstrated the usefulness of thioether-rich motifs¹¹⁸ in copper sensor design.¹¹⁸ Thioether-rich motifs have since been the ligand donor of choice for obtaining Cu(I) indicators with high selectivity. Fluorescence imaging of cells stained with CTAP-1 with exogenous supplementation with 150 μ M CuCl₂ for 12 h displayed a perinuclear staining pattern consistent with Golgi and mitochondrial localization, which was supported by immunofluorescence co-localization experiments. The fluorescence signal could be reversed by addition of the copper chelator 3,6-dithia-1,8-octanediol. XFM was interpreted to suggest co-localization of the CTAP-1 fluorescence and total copper and sulphur signals (Figure 4). From this starting point, systematic modifications to the fluorophore scaffold were employed to improve signal-to-noise response and to understand fundamental aspects of electron-transfer chemistry of these dyes in organic and aqueous media.^{109,119} In efforts to improve the hydrophilicity of these platforms, four hydroxymethyl groups were appended to the thiazacrown receptor and a sulphonate moiety to the fluorophore portion to produce CTAP-2 (Figure 3, Table 2).¹¹¹ This sensor could be dissolved directly in water instead of requiring dilution from an organic co-solvent, and it did not form nano-scale colloidal aggregates that commonly occur with fluorescent dyes. It is important to note that, while CTAP-1 and the BODIPY dyes CS1 and CS3 form colloids in solution, these solutions are still optically transparent, consisting of nanoparticles with sizes below the diffraction limit.¹²⁰ The primary application of CTAP-2 was in-gel fluorescence detection of Cu(I) bound to Atox1, suggesting that CTAP-2 may form a ternary complex with solvent-accessible, protein-bound Cu(I) ions. It was not indicated whether CTAP-2 exhibited a significant fluorescence turn-on response in solution in the presence of Cu(I)-Atox1, a result that

would support ternary complex formation given the substantial K_d difference between the probe and Atox1 (Tables 1 and 2).

4.2. BODIPY-based copper sensors

Our initial efforts in the development of fluorescent indicators for probing copper biology resulted in the first example of a visible excitation/emission probe for Cu(I), Coppersensor 1 (CS1, Figure 3, Table 2).^{112,121} CS1 consists of a boron dipyrromethene (BODIPY)-based fluorophore coupled to the acyclic form of the NS₄ receptor that we term NS₄'. In addition to a 10-fold turn-on response and high selectivity for copper with visible excitation at 540 nm and emission at 561 nm, CS1 responded to exogenous addition of 100 μ M CuCl₂ in HEK293T cells for 7 h in confocal imaging experiments. Moreover, addition of a copper chelator reversed the cellular fluorescence changes. The ability of CS1 to reversibly detect changes in labile copper in HEK293T cells was independently validated in a subsequent study,¹²² but application to detect labile Cu(I) changes in M17, U87MG, SH-SY5Y or CHO cell lines upon treatment with CuCl₂ or Cu(gtsm) were unsuccessful, reiterating a basic fact that a single chemical reagent cannot be used with the same efficacy in all biological sample types. Indeed, the first-generation CS1 probe has been employed effectively by other laboratories to investigate hyperaccumulation and misregulation of copper homeostasis in various bacterial,¹²³ yeast,¹²⁴⁻¹²⁶ and plant¹²⁷ models as a complementary technique to ICP-MS and traditional biochemical assays (Figure 4). For example, studies by Grass and co-workers show that increases in CS1 fluorescence are observed in bacterial¹²³ or yeast¹²⁴ upon exposure to copper surfaces, but not control stainless steel surfaces. Similarly, increases in CS1 staining in plants performed by Kramer and colleagues exposed to copper were subsequently used as pilot screens to identify new genes SPL7 and FRO4/5 that are involved in copper accumulation through the root,¹²⁷ which were then verified by genetic knockdown. In both cases, direct copper increases or decreases were verified by ICP-MS. Taken together, these studies highlight the value of validating a chemical probe in each new biological system with complementary bulk metal measurements, as well as genetic knockouts, to provide a coherent picture of metal homeostasis in that particular setting. Collecting such data is critical to elucidating what types of biological systems and situations are most suited for application of a given reagent.

In an effort to improve the signal-to-noise turn-on response of CS1, the fluoride substituents of the boron centre were replaced by more electron-rich methoxy groups (Figure 3, Table 2). This synthetic approach was inspired by Nagano and co-workers, who had elegantly shown that this substitution improves water solubility and decreases the driving force for donor PET quenching of the fluorophore by increasing its electron density.¹²⁸ The resulting probe, Coppersensor-3 (CS3), exhibits a markedly improved turn-on response (75-fold for CS3 over 10-fold for CS1) and a higher quantum yield for the Cu(I)-bound sensor ($\Phi = 0.40$ for CS3, $\Phi = 0.13$ for CS1) and maintains useful visible excitation/emission profiles. Moreover, the replacement of electron-poor fluorine substituents with electron-rich methoxy groups endows the fluorophore with greater binding affinity toward Cu(I) ($K_d = 9 \times 10^{-14}$ M for CS3, $K_d = 4 \times 10^{-12}$ M for CS1).⁴¹ The combination of improved turn-on response, quantum yield, and optical brightness, as well as tighter Cu(I) binding affinity, afforded for the first time the ability to visualize basal levels of labile copper in HEK293T cells that could be depleted by long-term treatment with the membrane-impermeable copper chelator bathocuproine disulphonate (BCS). These studies were supported by parallel XFM studies to directly confirm the observed decrease in cellular copper suggested by CS3, and subsequent studies have shown that CS3 can also

visualize increases in labile copper in other cell models upon copper supplementation (Figure 4).^{57,79} Application of CS3 to dissociated hippocampal neuronal cultures in initial screening studies showed that the CS3 fluorescence signal in resting neurons was largely localized to the cell soma rather than external dendritic regions under basal conditions. Upon depolarization by potassium chloride treatment, however, a significant increase in the dendritic fraction of total fluorescence intensity was observed, suggesting that copper pools in neurons were being redistributed upon inducing neural activity. These findings set the stage for XFM experiments, which were used to directly show that copper moves from somatic cell bodies to peripheral processes in neurons upon stimulation. Further studies using Ca(II) chelators and Ca(II) channel blockers with dual CS3 imaging and XFM strongly suggested that Ca(II) release is required for copper mobilization, linking the dynamics of this transition metal to canonical calcium signalling pathways. Since XFM is a low-throughput experiment, this study shows the biological value of using a fluorescent probe such as CS3 to more quickly screen conditions that could be applied to the direct metal imaging technique in fixed samples, with the added advantage of allowing for copper detection in live cells.

The application of CS3 to study copper in other biological models has also been reported (Figure 4). Two independent studies^{76,129} describe functions of CTR2, a homolog of the high-affinity copper transporter CTR1 that lacks much of the extracellular Met- and His-rich domain. Thiele and co-workers generated a CTR2^{-/-} mouse and used a combination of CS3 imaging and XFM to show the accumulation of copper-rich endosomal compartments in CTR2^{-/-} mouse fibroblasts and brain tissue, as well as the effect of truncation of CTR1 in reducing the number of these compartments.⁷⁶ These imaging experiments, which were supported by ICP-MS measurements directly showing copper accumulation upon knockout of CTR2, led to more extensive genetic and biochemical studies suggesting that truncation of CTR1 is key for copper mobilization from these endosomes, and that CTR2 plays a direct or indirect role in this process. In another study, the Howell laboratory applied two chemically distinct copper chelators (neocuproine and ammonium tetrathiomolybdate)¹³⁰ and genetic alteration of copper levels (overexpression and knockdown of CTR1, CTR2, ATP7A, and ATP7B) in a human epithelial cell type to show that treatments that deplete or increase intracellular copper levels as verified by ICP-MS track with relative CS3 fluorescence. *In vitro* studies also showed that CS3 fluorescence is not affected by the platinum antitumour drug cisplatin, pointing the way to the use of fluorescent copper indicators as potential screening tools to probe copper-dependent sensitivity to anticancer therapeutics, as CTR2 has been shown to regulate both the relative level of labile Cu(I) and sensitivity to cisplatin in a model of epithelial cancer. Polishchuk and co-workers utilized CS3 in screening assays and later confirmed using direct atomic absorption and ICP-MS analysis that endogenous ATP7B imports copper into lysosomes in hepatocytes in response to elevated copper levels.⁷⁹ More recently, Merchant and colleagues used CS3 in survey experiments to screen whether copper might be sequestered in zinc-deficient green algae *Chlamydomonas reinhardtii* cells.⁵⁷ These pilot data prompted further experiments with Nano-SIMS and X-ray absorption spectroscopy to identify a copper accumulating structure, termed a “cuprosome,” with a dynamic role in intracellular copper homeostasis. Reversible copper trafficking to these storage compartments may be a strategy for preventing protein mismetallation during zinc deficiency and enabling efficient cuproprotein re-metallation upon zinc resupply.

The aforementioned study also provides an opportunity to point out caveats of using fluorescent probes as screening tools for monitoring the availability and distribution of labile

copper pools and again emphasizes the value of combining both chemical and biological approaches to bear on a given system. This situation is particularly relevant to endosomal/lysosomal vesicles, which are emerging as important players in copper storage and transport.⁶³ Interpretation of any organic dye staining must be separated as best as possible from factors like membrane intercalation or acidic pH.⁵⁷ Any dyes or reagents that are hydrophobic are subject to this caution. In addition to verifying changes in copper pools by direct measurements such as ICP-MS, XFM, and Nano-SIMS, performing copper supplementation and chelation experiments to show reversibility, and performing genetic manipulations to copper-handling proteins, we introduced a control fluorescent probe to account for dye-dependent versus receptor-dependent fluorescent responses. In an initial design, we prepared the Control Coppensor-3 (Ctrl-CS3, Figure 3), which employs an identical fluorophore to CS3 and has the same number of receptor atoms, except that the four sulphur atoms required for metal binding are replaced by isosteric methylene groups lacking affinity for metals. Ctrl-CS3 does not respond to copper, and comparison between CS3 and Ctrl-CS3 in a series of spectroscopic control measurements show that CS3, but not Ctrl-CS3, can reversibly respond to Cu(I) in the presence of GSH, a model protein (bovine serum albumin, BSA), and model lipids (1,2-dimyristoyl-*sn*-glycero-3-phosphocholine, DMPC). Notably, the fluorescence of CS3 and its absolute turn-on response to Cu(I) is attenuated in the presence of these additives compared to pure aqueous buffer, but CS3 retains the relative ability to sense Cu(I) over Ctrl-CS3. This direct comparison between Cu(I)-responsive and non-responsive dyes is critical to separate dye-dependent versus receptor-dependent signals. Finally, although CS3 fluorescence is not constant between pH 3 to 8, it is Cu(I)-responsive over that entire range. Ctrl-CS3 was also used in cells to validate conclusions drawn from use of CS3. Confocal microscopy with *Chlamydomonas* cells versus control mutants lacking the copper regulon CRR1 show that CS3, but not Ctrl-CS3, is able to detect copper hyperaccumulation during zinc deficiency and that knockout of CRR1 ablates CS3 staining. Further control experiments with nitrogen-deficient *Chlamydomonas* cells, which accumulate lipids but do not hyperaccumulate copper, show staining with Nile Red, a general lipid marker, but not CS3, under the same experimental settings. The combined data from chemical and biological control experiments provide a coherent picture of copper homeostasis in this green algae system under the conditions used for this study, but it is important that the application of a reagent in each new experimental model is accompanied by controls in that model. In addition, the synergistic development of new probes and control reagents can strengthen the connection of the chemistry/biology interface.

4.3. A mitochondrial-targeted fluorescent copper indicator

A key challenge for fluorescent probe design is to develop new reagents that enable live-sample detection of labile metal pools localized to particular subcellular compartments. Owing to the importance of copper in the mitochondrion for aerobic respiration and antioxidant defence, our initial synthetic target was to devise a fluorescent reagent that could sense changes in availability of labile Cu(I) pools within this organelle. Mito-CS1¹¹³ combines a BODIPY-based copper sensor with a triphenylphosphonium moiety that is well established to effectively target cargo to mitochondria (Figure 3, Table 2).¹³¹ The synthetic copper sensing portion was derived from Ratio Coppensor-1 (RCS1), which was able to monitor ascorbate-induced changes in labile Cu(I) in live C6 cells but offered incremental value for imaging applications over CS3 owing to its longer multistep synthesis.¹³² Mito-CS1 localized to mitochondria in live HEK293T cells and fibroblasts and was responsive to both copper supplementation and copper chelation.

Control experiments with Rhodamine 123, a general dye for mitochondrial membrane potential, showed that this dye, unlike Mito-CS1, did not show changes in fluorescence upon addition or depletion of copper in the cell. Imaging with Mito-CS1 of fibroblasts derived from patients with mutations in the copper exporter ATP7A showed a relative increase in Mito-CS1 fluorescence that was confirmed by inductively coupled plasma optical emission spectroscopy showing copper hyperaccumulation. Mito-CS1 imaging of patient fibroblasts with mutations in mitochondrial copper metallochaperones SCO1 and SCO2 showed no difference in fluorescence signal compared to control fibroblasts. These imaging results are consistent with complementary ICP-OES measurements on those same SCO1/2 cells, which reveal a decrease in total copper compared to wildtype, but relatively constant mitochondrial copper in wildtype versus SCO1/2 mutants. Taken together, the combined Mito-CS1 and ICP-OES results indicate that the cell prioritizes homeostasis of total and labile mitochondrial copper levels even amid overall copper deficiency resulting from SCO1/2 mutation, presumably to preserve CcO and SOD activity.

4.4. Two-photon and near-infrared sensors for imaging copper in tissues and whole animals

Whereas fluorescent probes with visible-wavelength excitation and emission profiles are useful for microscopy of dissociated monolayers of cells, visible light poorly penetrates thicker specimens like tissue and whole animals. For this reason, the development of fluorescent copper sensors with longer wavelength near-infrared excitation profiles has been targeted for these applications. Cho and co-workers reported ACu1, a two-photon excitable probe for labile Cu(I) detection with a two photon absorption of 750 nm and cross section of 67 GM (Figure 3, Table 2).¹¹⁴ ACu1 fluorescence increases in cells upon copper supplementation, and chelation with NS₄' reverses the observed emission enhancement. The probe was also tested in rat hippocampal slices at a depth of 90-220 μm , in which treatment with CuCl₂ or NS₄' led to higher or lower observed fluorescence signals relative to untreated control samples, respectively.

Our laboratory developed Coppersensor-790 (CS790, Figure 3, Table 2)¹¹⁵ as a near-infrared sensor based on a cyanine 7 fluorophore, which has been used previously as a scaffold for constructing animal-compatible fluorescent probes for NO¹³³ and pH.¹³⁴ The sensor features excitation at 760 nm and emission at 790 nm with pK_a value of < 2, ensuring a pH-independent fluorescence response inside cells and animals. CS790 displays a ca. 15-fold turn-on response to Cu(I) *in vitro* and good metal ion selectivity. For cellular experiments, the carboxylates of the probe were capped with acetoxymethyl esters to yield CS790AM, which allows for greater membrane permeability and trapping in the cell via de-esterification by intracellular esterases.¹³⁵

CS790AM imaging in HEK293T cells showed relative increases in fluorescence intensity in cells pre-treated with CuCl₂ compared to control, and that addition of the copper chelator tris[2-(ethylthio)ethyl]amine (NS₃') fully reversed the observed fluorescence increases. CS790AM was then applied to imaging of visceral copper levels in live mice after peritoneal injection of the probe, representing the first example of live-mouse copper imaging with a fluorescent indicator (Figure 4). The measured CS790 fluorescence was ca. 10-fold over background autofluorescence with basal levels of copper, with further fluorescence increases observed upon treatment of mice with CuCl₂. Independent ICP-MS measurements showed a 4-fold increase in liver copper levels. Moreover, treatment with the copper chelator ATN-224, the choline salt of tetrathiomolybdate that is in development as a Wilson's disease treatment,¹³⁶ alone or in combination with CuCl₂, showed the expected reversible decreases in observed fluorescence. We then proceeded to utilize CS790AM to monitor peritoneal copper levels in ATP7B^{-/-} mice, a murine model for Wilson's

disease²¹ that shows aberrant elevations in copper levels in several tissues; in particular, the liver shows a 20- to 30-fold increase in copper accumulation compared to wildtype or heterozygous asymptomatic ATP7B^{+/-} mice as assessed by ICP-MS.^{115,137} CS790AM imaging in ATP7B^{+/-} mice results in a small but significant increase in peritoneal fluorescence relative to ATP7B^{+/-} mice, which was further verified by *ex vivo* tissue imaging of isolated liver, as well as in-gel filtration assays with serum that show that CS790 fluorescence tracks with direct detection of copper by atomic absorption in isolated fractions. Taken together, these data provide a promising start for the potential application of copper sensors to study physiology, diagnose disease, and monitor treatment of copper misregulation in animals. Along the same lines, Wan and co-workers reported a related sensor, Cu(I) probe 3, consisting of NS₄' coupled to directly to a cyanine fluorophore.¹¹⁶ This sensor has been applied to visualize ascorbic acid-stimulated increases in labile Cu(I) in cells.

4.5. Rhodol-based copper fluorophores

To increase the utility of chemical fluorescent probes for the study of biological copper, we sought to expand synthetic efforts to new scaffolds. Noting that the original BODIPY sensors, although useful in many settings because of their high selectivity and biologically compatible visible wavelength excitation/emission profiles, were limited in some cases by their high hydrophobicity, insufficient photostability for prolonged imaging, and relatively short shelf life.⁵⁷ We sought to both improve these properties and prepare sensors that could be used in one- or two-photon microscopy for application in cell and tissue specimens. In a first step toward these goals, we recently synthesized a family of new fluorescent copper sensors based on the hybrid fluorescein-rhodamine rhodol fluorophore,¹³⁸ which offers a combination of improved hydrophilicity and photostability, tuneable visible excitation/emission profiles and signal-to-noise responses, photostability, and the ability to undergo effective one- or two-photon excitation. Of the five initial targets made, Copper Rhodol 3 (CR3) was the best performing dye in the series, exhibiting a 13-fold turn-on response to Cu(I) binding *in vitro* (Figure 3).⁴³ The substitution of a methyl group on the pendant aryl ring with a more bulky trifluoromethyl group afforded Copper Fluor-3 (CF3, Figure 3). This CH₃ to CF₃ substitution serves two purposes; first, it minimizes non-radiative decay from aryl-aryl rotations that may limit quantum yields, and second, it favours PET quenching in the unbound state by withdrawing electron density from the aryl ring. As a result, CF3 exhibited improvements in quantum yield and turn-on responses to Cu(I) compared to CR3 (Table 2), yielding a 40-fold emission enhancement. The improved hydrophilicities of CR3 and CF3 over CS3 were confirmed by measurements of apparent octanol/water partition coefficient values (logD values of 0.96, 1.15, and 3.46, respectively, where smaller values indicate greater hydrophilicity). Finally, following the development of Ctrl-CS3,⁵⁷ the analogous Ctrl-CR3 and Ctrl-CF3 dyes were synthesized. We performed a series of *in vitro* experiments to show that CF3, but not Ctrl-CF3, is capable of reversibly sensing Cu(I) in the presence of model protein (BSA), two liposome models, and GSH. Moreover, as a more faithful *in vitro* mimic of the cellular environment, we demonstrated that CF3, but not Ctrl-CF3, was able to reversibly detect addition of Cu(I) in anaerobic HEK293T cell lysates. The collective data establish that CF3 is capable of responding reversibly to Cu(I) even in the presence of potentially complicating cellular components.

CF3 was used for one- and two-photon imaging of dissociated hippocampal neuronal cultures and retinal tissue. Short-term application of the membrane-impermeable copper chelator BCS leads to measurable on-stage decreases in CF3 fluorescence intensity in neurons and in

tissue, suggesting a depletion of labile Cu(I) within that timeframe. In contrast, these treatments had minimal effect on Ctrl-CF3 fluorescence. We note that this behaviour can be cell-type dependent, as we have not observed such rapid responses to BCS treatments in all models. Nevertheless, the data are consistent with work by Gitlin noting a rapid copper-independent mobilization of ATP7A from the Golgi to plasma membrane in <10 min in neurons in response to NMDA receptor activation.¹³⁹ Further imaging studies using heterozygous CTR1^{+/-} mice that show decreased levels of brain copper by ICP-MS are consistent with the notion that CF3, but not Ctrl-CF3, is capable of distinguishing normal levels of labile Cu(I) in wildtype mice compared to depletion of labile Cu(I) in the CTR1^{+/-} mutant mice.

We then sought to test the effects of altering labile copper pools by pharmacology with copper chelators (BCS, ATN-224) or genetic manipulation (CTR1 knockdown) on spontaneous activity of neural circuits. These treatments established that targeted attenuation of labile copper alters the spatiotemporal properties of spontaneous activity in developing hippocampal and retinal circuits. Taken together, the data identify an essential role for copper in a key neural function and suggest broader contributions of this transition metal to cell signalling pathways.

4.6 Reaction-based fluorescent copper probes

An attractive alternative strategy to probe biological copper is to exploit reaction, rather than reversible recognition, as a way to promote selective analyte detection.¹⁴⁰ Taki and colleagues harnessed the reactivity of Cu(I) with O₂ to create FluTPA1, the first reaction-based sensor for Cu(I), by combining a reduced fluorescein-type dye capped with a tetradentate tris[(2-pyridyl)-methyl]amine ligand for copper (Figure 3, Table 2).¹¹⁷ Upon Cu(I) binding and reaction under aerobic conditions, the benzyl ether C-O bond is cleaved and oxidation liberates fluorescein. The probe exhibits a >1500-fold turn-on after 2 h reaction under the reported experimental conditions and responds to Cu(II) addition in HeLa cells. We note that relatively slow reaction kinetics are useful for cellular studies to prevent probe fluorescence from being saturated in all conditions for reagents of this type. Moreover, cross-reactivity with Fe(II), another metal ion with a labile pool inside the cell, is minor as shown by *in vitro* studies. While the irreversible reaction-based trigger brings selectivity and sensitivity, it also may limit temporal and spatial resolution. In an effort to improve the latter concern, a recent attempt to use a triphenylphosphonium moiety to target the probe to mitochondria resulted in primarily lysosomal localization and significantly higher reactivity with Co(II) and Fe(II) compared to the parent probe.¹⁴¹ Inspired by FluTPA1, our laboratory has exploited O₂-dependent reaction-based approaches to detection of Co(II)¹⁴² and Fe(II),¹⁴³ two redox-active metals that are potent quenchers and thus difficult to detect in a turn-on mode by traditional binding and recognition strategies.

5. Concluding Remarks

Fluorescent chemical probes offer a powerful set of reagents for probing the biology of copper as an essential element for life. These chemical tools are most effectively employed to probe the availability, localization, and dynamics of labile Cu(I) in living systems from the subcellular to whole-animal level. This technology for detection of labile copper in live samples offers a complementary approach to the direct measurement techniques for total copper in fixed samples such as ICP-MS, XFM/micro-XANES, and Nano-SIMS. The higher-throughput nature of molecular imaging with fluorescent chemical probes compared to these bulk measurement techniques fulfils an important biological and potentially clinical need by facilitating pilot

screens that can lead to more rigorous and in-depth biological inquiries. Indeed, this approach has proved useful in a diverse array of biological systems – ranging from bacteria and yeast, to algae and plants, to various mammalian cells and tissues – that have already been interrogated by a relatively small set of chemical probes. Because the synthetic chemistry and technology development for Cu(I) probes is in its infancy compared to the traditional and broadly-useful fluorescent indicators for Ca(II) and Zn(II), a number exciting possibilities remain open for exploration. Like any reagents, including chemical chelators and isolated proteins, the relative responses to Cu(I) may be condition-dependent, so absolute measurements made under carefully restricted *in vitro* conditions must not be over-interpreted when applied to biological systems that are inherently heterogeneous. Rigorous *in vitro* chemical characterization to demonstrate that probes can reversibly respond to Cu(I) in the presence of biological components, or even in cell lysates, together with accompanying direct metal measurements (ICP-MS, XFM, Nano-SIMS, etc.) and genetic controls, can be used in concert to support the application of a chemical reagent to help explore and understand this biology.

Advances in our understanding of underlying photophysics, increasing signal-to-noise contrast, tuning of wavelength profiles to the visible and near-infrared range for more effective application to cellular and animal systems, improving dye hydrophilicity, and developing control compounds to distinguish between dye-dependent and metal receptor-dependent fluorescence responses have facilitated broad utilization of chemical probes in a variety of aforementioned biological applications. In addition to further improvements of the aforementioned properties, other exciting opportunities to pursue by synthetic design include:

1) *Expanding the K_d range available.* The vast majority of synthetic sensors fall within the 10^{-10} to 10^{-13} M range, whereas the other major class of Cu(I) probes, genetically encoded sensors, fall within the 10^{-18} to 10^{-21} M range.¹⁴⁴⁻¹⁴⁷ Many interesting protein ligands in the cell lie in between these windows. A challenge of developing tighter-binding probes is the potential for probe saturation by more weakly bound copper pools (e.g. the GSH-bound pool with which the existing sensors may be equilibrating in the cell). Therefore, design of sensors able to form ternary complexes with Cu(I) bound to specific cellular ligands such as Atox1 is an intriguing avenue of research.

2) *Designing ratiometric probes.* While development of control probes is an important step forward, ratiometric probes¹⁴⁸ serve as their own internal controls to correct for potential dye-dependent localization and sample thickness effects. Such sensors may also allow for more quantitative assessment of the concentrations at which Cu(I) is buffered in the cell. In the meantime, further improvements to the control sensors would contribute to their utility in cells. Ctrl-CS3 and Ctrl-CF3 are dim owing to PET quenching, and control sensors with fluorescence properties more similar to the “on-state” of their parent sensors would enable even more sensitive control experiments.

3) *Directing probes to particular cell types or subcellular locales.* Organelles of particular interest include the mitochondrion, nucleus, Golgi, and lysosomes. Using currently available technology, genetically encoded sensors tend to be more easily rationally directed to particular subcellular locations than synthetic probes, offering an attractive path forward for targeting.¹⁴⁸⁻¹⁵¹

4) *Detection of Cu(II)*. The inherent quenching properties of Cu(II), which is paramagnetic in any coordination geometry, has made the development of turn-on or wavelength-shifting fluorescent sensors challenging. Reaction-based schemes, which have been used successfully for Cu(I), may be useful for overcoming these difficulties.

To close, the discovery of new copper-accumulating organelles, roles for labile copper in a fundamental property of neural circuits, and first steps toward a potential non-invasive diagnostic for genetic copper disorders represent but a few of the biological lessons that have been illuminated using these chemical reagents. Continued innovations in the development of fluorescent chemical probes, in conjunction with an open spirit of collaboration between chemists, biologists, and clinicians will certainly uncover novel metal biology in living systems with the potential to lead to new therapeutics and diagnostics.

Acknowledgements

We thank the National Institutes of Health (GM 79465) for supporting our work on copper imaging probes. C.J.C. is an Investigator of the Howard Hughes Medical Institute. J.A.C. is supported by a postdoctoral fellowship from the Jane Coffin Childs Memorial Fund for Medical Research, A.T.A. is supported by an NSF Predoctoral Fellowship, and A.T.A. and K.M.R.T. were partially supported by a Chemical Biology Training Grant from the NIH (T32 GM066698).

References

1. S. J. Lippard, J. M. Berg and C. University Science Books: Mill Valley, *Principles of Bioinorganic Chemistry*. University Science Books: Mill Valley, CA, 1994.
2. R. R. Crichton and J. L. Pierre, *Biomaterials*, 2001, **14**, 99-112.
3. P. G. Ridge, Y. Zhang and V. N. Gladyshev, *PLoS One*, 2008, **3**, e1378.
4. A. K. Boal and A. C. Rosenzweig, *Chem. Rev.*, 2009, **109**, 4760-4779.
5. S. Ferguson-Miller and G. T. Babcock, *Chem. Rev.*, 1996, **96**, 2889-2908.
6. S. Ishida, P. Andreux, C. Poitry-Yamate, J. Auwerx and D. Hanahan, *Proc. Natl. Acad. Sci. U.S.A.*, 2013, **110**, 19507-19512.
7. A. Ghosh, P. P. Trivedi, S. A. Timbalia, A. T. Griffin, J. J. Rahn, S. S. Chan and V. M. Gohil, *Hum. Mol. Genet.*, 2014, **23**, 3596-3606.
8. N. E. Hellman and J. D. Gitlin, *Annu. Rev. Nutr.*, 2002, **22**, 439-458.
9. C. Olivares and F. Solano, *Pigment Cell Melanoma Res.*, 2009, **22**, 750-760.
10. J. M. McCord and I. Fridovich, *J. Biol. Chem.*, 1969, **244**, 6049-6055.
11. P. J. Hart, M. M. Balbirnie, N. L. Ogihara, A. M. Nersissian, M. S. Weiss, J. S. Valentine and D. Eisenberg, *Biochemistry*, 1999, **38**, 2167-2178.
12. B. R. Roberts, J. A. Tainer, E. D. Getzoff, D. A. Malencik, S. R. Anderson, V. C. Bomben, K. R. Meyers, P. A. Karplus and J. S. Beckman, *J. Mol. Biol.*, 2007, **373**, 877-890.
13. A. R. Reddi and V. C. Culotta, *Cell*, 2013, **152**, 224-235.
14. I. Fridovich, *Annu. Rev. Biochem.*, 1995, **64**, 97-112.
15. N. Herranz, N. Dave, A. Millanes-Romero, L. Morey, V. M. Diaz, V. Lorenz-Fonfria, R. Gutierrez-Gallego, C. Jeronimo, L. Di Croce, A. G. de Herreros and S. Peiro, *Mol. Cell*, 2012, **46**, 369-376.
16. H. C. P. Dawkes, S. E. V., *Curr. Opin. in Struct. Biol.*, 2001, **11**, 666-673.
17. J. P. Klinman, *Biochim. Biophys. Acta*, 2003, **1637**, 131-137.

18. C. Vulpe, B. Levinson, S. Whitney, S. Packman and J. Gitschier, *Nat. Genet.*, 1993, **3**, 7-13.
19. S. G. Kaler, *Nat. Rev. Neurol.*, 2011, **7**, 15-29.
20. S. La Fontaine and J. F. Mercer, *Arch. Biochem. Biophys.*, 2007, **463**, 149-167.
21. S. Lutsenko, *Biochem. Soc. Trans.*, 2008, **36**, 1233-8.
22. D. Huster, M. Hoppert, S. Lutsenko, J. Zinke, C. Lehmann, J. Mossner, F. Berr and K. Caca, *Gastroenterology*, 2003, **124**, 335-345.
23. D. Huster, *Ann. NY Acad. Sci.*, 2014, **1314**, 37-44.
24. E. L. Que, D. W. Domaille and C. J. Chang, *Chem. Rev.*, 2008, **108**, 1517-49.
25. S. Ayton, P. Lei and A. I. Bush, *Free Radic. Biol. Med.*, 2013, **62**, 76-89.
26. K. J. Barnham, C. L. Masters and A. I. Bush, *Nat. Rev. Drug Discov.*, 2004, **3**, 205-14.
27. M. G. Savelieff, S. Lee, Y. Liu and M. H. Lim, *ACS Chem. Biol.*, 2013, **8**, 856-865.
28. K. E. Matlack, D. F. Tardiff, P. Narayan, S. Hamamichi, K. A. Caldwell, G. A. Caldwell and S. Lindquist, *Proc. Natl. Acad. Sci. U.S.A.*, 2014, **111**, 4013-4018.
29. W. I. Vonk, V. Kakkar, P. Bartuzi, D. Jaarsma, R. Berger, M. H. Hofker, L. W. Klomp, C. Wijmenga, H. H. Kampinga and B. van de Sluis, *PLoS One*, 2014, **9**, e92408.
30. P. Davies, P. C. McHugh, V. J. Hammond, F. Marken and D. R. Brown, *Biochemistry*, 2011, **50**, 10781-10791.
31. A. J. McDonald, J. P. Dibble, E. G. Evans and G. L. Millhauser, *J. Biol. Chem.*, 2014, **289**, 803-813.
32. G. Xiao, Q. Fan, X. Wang and B. Zhou, *Proc. Natl. Acad. Sci. U.S.A.*, 2013, **110**, 14995-15000.
33. L. J. Hayward, J. A. Rodriguez, J. W. Kim, A. Tiwari, J. J. Goto, D. E. Cabelli, J. S. Valentine and R. H. J. Brown, *J. Biol. Chem.*, 2002, **277**, 15923-15931.
34. J. L. Burkhead and S. Lutsenko, in *Lipid Metabolism*, ed. R. V. Baez. InTech, 2013, DOI: 10.5772/51819.
35. D. Huster, T. D. Purnat, J. L. Burkhead, M. Ralle, O. Fiehn, F. Stuckert, N. E. Olson, D. Teupser and S. Lutsenko, *J. Biol. Chem.*, 2007, **282**, 8343-8355.
36. D. Huster and S. Lutsenko, *Mol. Biosyst.*, 2007, **3**, 816-824.
37. T. E. Engle, *J. Anim. Sci.*, 2011, **89**, 591-596.
38. T. S. Nielsen, N. Jessen, J. O. Jorgensen, N. Moller and S. Lund, *J. Mol. Endocrinol.*, 2014, **52**, R199-R222.
39. M. L. Turski, D. C. Brady, H. J. Kim, B. E. Kim, Y. Nose, C. M. Counter, D. R. Winge and D. J. Thiele, *Mol. Cell. Biol.*, 2012, **32**, 1284-1295.
40. D. C. Brady, M. S. Crowe, M. L. Turski, G. A. Hobbs, X. Yao, A. Chaikuad, S. Knapp, K. Xiao, S. L. Campbell, D. J. Thiele and C. M. Counter, *Nature*, 2014, **509**, 492-496.
41. S. C. Dodani, D. W. Domaille, C. I. Nam, E. W. Miller, L. A. Finney, S. Vogt and C. J. Chang, *Proc. Natl. Acad. Sci. U.S.A.*, 2011, **108**, 5980-5.
42. D. E. B. Hartter, A., *Synapse*, 1988, **2**, 412-415.
43. S. C. Dodani, A. Firl, J. Chan, C. I. Nam, A. T. Aron, C. S. Onak, K. M. Ramos-Torres, J. Paek, C. M. Webster, M. B. Feller and C. J. Chang, *Proc. Natl. Acad. Sci. U.S.A.*, 2014, **111**, 16280-16285.
44. L. Yang, R. McRae, M. M. Henary, R. Patel, B. Lai, S. Vogt and C. J. Fahrni, *Proc. Natl. Acad. Sci. U.S.A.*, 2005, **102**, 11179-84.
45. R. P. Patel, J. McAndrew, H. Sellak, C. R. White, H. Jo, B. A. Freeman and V. M. Darley-Usmar, *Biochim. Biophys. Acta*, 1999, **1411**, 385-400.

46. B. Halliwell and J. M. C. Gutteridge, *Biochem. J.*, 1984, **219**, 1-14.
47. C. E. Outten and T. V. O'Halloran, *Science*, 2001, **292**, 2488-2492.
48. J. Lee, M. J. Petris and D. J. Thiele, *J. Biol. Chem.*, 2002, **277**, 40253-20259.
49. I. Hamza, J. Prohaska and J. D. Gitlin, *Proc. Natl. Acad. Sci. U.S.A.*, 2003, **100**, 1215-1220.
50. R. McRae, B. Lai and C. J. Fahrni, *J. Biol. Inorg. Chem.*, 2010, **15**, 99-105.
51. S. Vogt and M. Ralle, *Anal. Bioanal. Chem.*, 2013, **405**, 1809-20.
52. M. D. de Jonge and S. Vogt, *Curr. Opin. Struct. Biol.*, 2010, **20**, 606-14.
53. L. Finney, S. Mandava, L. Ursos, W. Zhang, D. Rodi, S. Vogt, D. Legnini, J. Maser, F. Ikpatt, O. I. Olopade and D. Glesne, *Proc Natl Acad Sci U S A*, 2007, **104**, 2247-52.
54. R. McRae, B. Lai and C. J. Fahrni, *Metallomics*, 2013, **5**, 52-61.
55. D. Bourassa, S. C. Gleber, S. Vogt, H. Yi, F. Will, H. Richter, C. H. Shin and C. J. Fahrni, *Metallomics*, 2014, **6**, 1648-55.
56. L. Finney, Y. Chishti, T. Khare, C. Giometti, A. Levina, P. A. Lay and S. Vogt, *ACS Chem. Biol.*, 2010, **5**, 577-87.
57. A. Hong-Hermesdorf, M. Miethke, S. D. Gallaher, J. Kropat, S. C. Dodani, J. Chan, D. Barupala, D. W. Domaille, D. I. Shirasaki, J. A. Loo, P. K. Weber, J. Pett-Ridge, T. L. Stemmler, C. J. Chang and S. S. Merchant, *Nat. Chem. Biol.*, 2014, **10**, 1034-1042.
58. J. S. Becker, A. Matusch and B. Wu, *Anal. Chem. Acta*, 2014, **835**, 1-18.
59. A. C. Rosenzweig and T. V. O'Halloran, *Curr. Opin. Chem. Biol.*, 2000, **4**, 140-147.
60. N. J. Robinson and D. R. Winge, *Annu. Rev. Biochem.*, 2010, **79**, 537-62.
61. S. Lutsenko, *Curr. Opin. Chem. Biol.*, 2010, **14**, 211-7.
62. S. Tottey, K. J. Waldron, S. J. Firbank, B. Reale, C. Bessant, K. Sato, T. R. Cheek, J. Gray, M. J. Banfield, C. Dennison and N. J. Robinson, *Nature*, 2008, **455**, 1138-1142.
63. C. E. Blaby-Haas and S. S. Merchant, *J. Biol. Chem.*, 2014, **289**, 28129-28136.
64. L. Banci, I. Bertini, S. Ciofi-Baffoni, T. Kozyreva, K. Zovo and P. Palumaa, *Nature*, 2010, **465**, 645-8.
65. Z. Xiao, J. Brose, S. Schimo, S. M. Ackland, S. La Fontaine and A. G. Wedd, *J. Biol. Chem.*, 2011, **286**, 11047-55.
66. Z. Xiao, L. Gottschlich, R. van der Meulen, S. R. Udagedara and A. G. Wedd, *Metallomics*, 2013, **5**, 501-13.
67. Y. Furukawa, A. S. Torres and T. V. O'Halloran, *EMBO J.*, 2004, **23**, 2872-81.
68. J. Finney, H. J. Moon, T. Ronnebaum, M. Lantz and M. Mure, *Arch Biochem Biophys*, **546**, 19-32.
69. A. Meister, in *The Liver: Biology and Pathobiology: Second Edition*, ed. I. M. Aria, H. Popper, D. Schachter, D. A. Shafritz. Raven Press, New York, 1988.
70. A. Corazza, I. Harvey and P. J. Sadler, *Eur. J. Biochem.*, 1996, **136**, 697-705.
71. A. Kr zel, W. Lesniak, M. Jezowska-Bojczuk, P. Mlynarz, J. Brasun, H. Kozlowski and W. Bal, *J Inorg Biochem*, 2001, **84**, 77-88.
72. S. Puig, J. Lee, M. Lau and D. J. Thiele, *J. Biol. Chem.*, 2002, **277**, 26021-26030.
73. J. T. Rubino, P. Riggs-Gelasco and K. J. Franz, *J. Biol. Inorg. Chem.*, 2010, **15**, 1033-1049.
74. C. R. Pope, A. G. Flores, J. H. Kaplan and V. M. Unger, *Curr. Top. Membr.*, 2012, **69**, 97-112.
75. A. V. Davis and T. V. O'Halloran, *Nat. Chem. Biol.*, 2008, **4**, 148-151.

76. H. Ohrvik, Y. Nose, L. K. Wood, B. E. Kim, S. C. Gleber, M. Ralle and D. J. Thiele, *Proc. Natl. Acad. Sci. U.S.A.*, 2013, **110**, E4279-E4288.
77. S. Lutsenko, N. L. Barnes, M. Y. Bartee and O. Y. Dmitriev, *Physiol. Rev.*, 2007, **87**, 1011-1046.
78. L. B. Banci, I.; Calderone, V.; Della-Malva, N.; Felli, I. C.; Neri, S.; Pavelkova, A.; Rosato, A., *Biochem. J.*, 2009, **422**, 37-42.
79. E. V. Polishchuk, M. Concilli, S. Iacobacci, G. Chesi, N. Pastore, P. Piccolo, S. Paladino, D. Baldantoni, S. C. van Ijzendoorn, J. Chan, C. J. Chang, A. Amoresano, F. Pane, P. Pucci, A. Tarallo, G. Parenti, N. Brunetti-Pierri, C. Settembre, A. Ballabio and R. S. Polishchuk, *Dev. Cell*, 2014, doi: 10.1016/j.devcel.2014.04.033.
80. D. E. K. Sutherland and M. J. Stillman, *Metallomics*, 2011, **3**, 444-463.
81. S. C. C. Leary, P. A.; Kaufman, B. A.; Guercin, G. H.; Mattman, A.; Palaty, J.; Lockitch, G.; Winge, D. R.; Rustin, P.; Horvath, R.; Shoubridge, E. A. , *Cell Metab.*, 2007, **5**, 9-20.
82. S. C. Leary, P. A. Cobine, T. Nishimura, R. M. Verdijk, R. de Krijger, R. de Coo, M. A. Tarnopolsky, D. R. Winge and E. A. Shoubridge, *Mol. Biol. Cell*, 2013, **24**, 683-691.
83. A. T. Ghosh, P. P. ; Timbalia, S. A. ; Griffin, A. T. ; Rahn, J. J. ; Chan, S. S. ; Gohil, V. M., *Hum. Mol. Genet.*, 2014, **23**, 3596-3606.
84. P. A. Cobine, L. D. Ojeda, K. M. Rigby and D. R. Winge, *J. Biol. Chem.*, 2004, **279**, 14447-55.
85. P. A. Cobine, F. Pierrel, M. L. Bestwick and D. R. Winge, *J. Biol. Chem.*, 2006, **281**, 36552-9.
86. E. B. Maryon, S. A. Molloy and J. H. Kaplan, *Am. J. Physiol. Cell. Physiol.*, 2013, **304**, C768-C779.
87. R. L. McNaughton, A. R. Reddi, M. H. S. Clement, A. Sharma, K. Barnese, L. Rosenfeld, E. B. Gralla, J. S. Valentine, V. C. Culotta and B. M. Hoffman, *Proc. Natl. Acad. Sci. U. S. A.*, 2010, **107**, 15335-15339.
88. M. Lafontan, in *Adipose Tissue in Health and Disease*, ed. T. Leff, J. G. Granneman. Wiley-VCH Verlag GmbH & Co: KGaA, Weinheim, Germany, 2010.
89. D. W. Q. Domaille, E. L. ; Chang, C. J., *Nat. Chem. Biol.*, 2008, **4**, 168-175.
90. V. A. Rapisarda, S. I. Volentini, R. N. Farias and E. M. Massa, *Anal. Biochem.*, 2002, **307**, 105-9.
91. R. Y. Tsien, *Biochemistry*, 1980, **19**, 2396-2404.
92. C. J. L. Chang, S. J. , *Met. Ions Life Sci.* , 2006, **1**, 321-370.
93. E. M. L. Nolan, S. J. , *Acc. Chem. Res.*, 2009, **42**, 193-203.
94. M. D. T. Pluth, E.; Lippard, S. J., *Annu. Rev. Biochem.*, 2011, **80**, 333-335.
95. C. J. K. Frederickson, E. J.; Ringo, D.; Frederickson, R. E. J., *J. Neurosci. Methods*, 1987, **20**, 91-103.
96. P. D. F. Zalewski, I. J.; Betts, W. H., *Biochem J.*, 1993, **296**, 403-408.
97. G. P. Gryniewicz, M. ; Tsien, R. Y. , *J. Biol. Chem.*, 1985, **250**, 3440-3450.
98. A. P. de Silva, T. S. Moody and G. D. Wright, *Analyst*, 2009, **134**, 2385-93.
99. A. P. G. de Silva, H. Q. N. ; Gunnlaugsson, T. ; Huxley, A. J. M. ; McCoy, C. P. ; Rademacher, J. T. ; Rice, T. E. , *Chem. Rev.*, 1997, **97**, 1515-1566.
100. A. W. Czarnik, *Acc. Chem. Res.*, 1994, **27**, 302-308.
101. H. N. Kojima, N.; Kikuchi, K.; Kawahara, S.; Kirino, Y.; Nagoshi, H.; Hirata, Y.; Nagano, T., *Anal. Chem.*, 1998, **70**, 2446-2453.

102. K. M. Tanaka, T. ; Umezawa, N. ; Urano, Y. ; Kikuchi, K. ; Higuchi, T. ; Nagano, T., *J. Am. Chem. Soc.*, 2001, **123**, 2530-2536.
103. Y. Urano, M. Kamiya, K. Kanda, T. Ueno, K. Hirose and T. Nagano, *J. Am. Chem. Soc.*, 2005, **127**, 4888-94.
104. A. Weller, *Pure Appl. Chem.*, 1968, **16**, 115-124.
105. D. Rehm and A. Weller, *Isr. J. Chem.*, 1970, **8**, 259-271.
106. N. Boens, V. Leen and W. Dehaen, *Chem. Soc. Rev.*, 2012, **41**, 1130-72.
107. T. Ueno, Y. Urano, K. Setsukinai, H. Takakusa, H. Kojima, K. Kikuchi, K. Ohkubo, S. Fukuzumi and T. Nagano, *J. Am. Chem. Soc.*, 2004, **126**, 14079-85.
108. C. J. Fahrni, L. Yang and D. G. VanDerveer, *J. Am. Chem. Soc.*, 2003, **125**, 3799-812.
109. A. F. Chaudhry, M. Verma, M. T. Morgan, M. M. Henary, N. Siegel, J. M. Hales, J. W. Perry and C. J. Fahrni, *J. Am. Chem. Soc.*, 2010, **132**, 737-47.
110. T. U. Ueno, Y.; Setsukinai, K.; Takakusa, H.; Kojima, H.; Kikuchi, K.; Ohkubo, K.; Fukuzumi, S.; Nagano, T., *J. Am. Chem. Soc.*, 2004, **126**, 14079-14085.
111. M. T. Morgan, P. Bagchi and C. J. Fahrni, *J. Am. Chem. Soc.*, 2011, **133**, 15906-15909.
112. L. Zeng, E. W. Miller, A. Pralle, E. Y. Isacoff and C. J. Chang, *J. Am. Chem. Soc.*, 2006, **128**, 10-11.
113. S. C. Dodani, S. C. Leary, P. A. Cobine, D. R. Winge and C. J. Chang, *J. Am. Chem. Soc.*, 2011, **133**, 8606-16.
114. C. S. Lim, J. H. Han, C. W. Kim, M. Y. Kang, D. W. Kang and B. R. Cho, *Chem. Commun. (Camb.)*, 2011, **47**, 7146-7148.
115. T. Hirayama, G. C. Van de Bittner, L. W. Gray, S. Lutsenko and C. J. Chang, *Proc. Natl. Acad. Sci. U.S.A.*, 2012, **109**, 2228-33.
116. X. Cao, W. Lin and W. Wan, *Chem. Commun. (Camb.)*, 2012, **48**, 6247-6249.
117. M. Taki, S. Iyoshi, A. Ojida, I. Hamachi and Y. Yamamoto, *J. Am. Chem. Soc.*, 2010, **132**, 5938-5939.
118. M. M. Bernardo, M. J. Heeg, R. R. Schroeder, L. A. Ochrymowycz and D. B. Rorabacher, *Inorg. Chem.*, 1992, **31**, 191-198.
119. A. F. M. Chaudhry, S.; Hardcastle, K.; Fahrni, C. J., *Chem. Sci.*, 2011, **2**, 1016-1024.
120. C. J. Fahrni, *Curr. Opin. Chem. Biol.*, 2013, **17**, 656-662.
121. E. W. Miller, L. Zeng, D. W. Domaille and C. J. Chang, *Nat. Protoc.*, 2006, **1**, 824-827.
122. K. A. Price, J. L. Hickey, Z. Xiao, A. G. Wedd, S. A. James, J. R. Liddell, P. J. Crouch, A. R. White and P. S. Donnelly, *Chem. Sci.*, 2012, **3**, 2748-2759.
123. C. Espirito Santo, E. W. Lam, C. G. Elowsky, D. Quaranta, D. W. Domaille, C. J. Chang and G. Grass, *Appl. Environ. Microbiol.*, 2011, **77**, 794-802.
124. D. Quaranta, T. Krans, C. Espirito Santo, C. G. Elowsky, D. W. Domaille, C. J. Chang and G. Grass, *Appl. Environ. Microbiol.*, 2011, **77**, 416-426.
125. K. D. Cusick, S. C. Minkin, S. C. Dodani, C. J. Chang, S. W. Wilhelm and G. S. Saylor, *Environ. Sci. Technol.*, 2012, **46**, 2959-2966.
126. J. Beaudoin, R. Ioannoni, L. López-Maury, J. Bähler, S. Ait-Mohand, B. Guérin, S. C. Dodani, C. J. Chang and S. Labbé, *J. Biol. Chem.*, 2011, **286**, 34356-34372.
127. M. Bernal, D. Casero, V. Singh, G. T. Wilson, A. Grande, H. Yang, S. C. Dodani, M. Pellegrini, P. Huijser, E. L. Connolly, S. S. Merchant and U. Kramer, *Plant Cell*, 2012, **24**, 738-761.
128. Y. Gabe, T. Ueno, Y. Urano, H. Kojima and T. Nagano, *Anal. Bioanal. Chem.*, 2006, **386**, 621-6.

129. C. P. Huang, M. Fofana, J. Chan, C. J. Chang and S. B. Howell, *Metallomics*, 2014, **6**, 654-661.
130. X. Ding, H. Xie and Y. J. Kang, *J. Nutr. Biochem.*, 2011, **22**, 301-310.
131. R. A. J. Smith, C. M. Porteous, A. M. Gane and M. P. Murphy, *Proc. Natl. Acad. Sci. USA*, 2003, **100**, 5407-5412.
132. D. W. Domaille, L. Zeng and C. J. Chang, *J. Am. Chem. Soc.*, 2010, **132**, 1194-1195.
133. E. Sasaki, H. Kojima, H. Nishimatsu, Y. Urano, K. Kikuchi, Y. Hirata and T. Nagano, *J. Am. Chem. Soc.*, 2005, **127**, 3684-3685.
134. S. A. Hilderbrand and R. Weissleder, *Chem. Commun. (Camb.)*, 2007, 2747-2749.
135. R. Y. Tsien, *Nature*, 1981, **290**, 527-528.
136. G. J. Brewer, *Metallomics*, 2009, **1**, 199-206.
137. D. Huster, M. J. Finegold, C. T. Morgan, J. L. Burkhead, R. Nixon, S. M. Vanderwerf, C. T. Gilliam and S. Lutsenko, *Am. J. Pathol.*, 2006, **168**, 423-34.
138. J. E. Whitaker, R. P. Haugland, D. Ryan, P. C. Hewitt, R. P. Haugland and F. G. Prendergast, *Anal. Biochem.*, 1992, **207**, 267-279.
139. M. L. Schlieff, A. M. Craig and J. D. Gitlin, *J. Neurosci.*, 2005, **25**, 239-46.
140. J. Chan, S. C. Dodani and C. J. Chang, *Nat. Chem.*, 2012, **4**, 973-984.
141. M. Taki, K. Akaoka, K. Mitsui and Y. Yamamoto, *Org. Biomol. Chem.*, 2014, **12**, 4999-5005.
142. H. Y. N. Au-Yeung, E. J.; Chang, C. J., *Chem. Commun.*, 2012, **48**, 5268-5270.
143. H. Y. Au-Yeung, J. Chan, T. Chantarojsiri and C. J. Chang, *J. Am. Chem. Soc.*, 2013, **135**, 15165-73.
144. S. V. Wegner, H. Arslan, M. Sunbul, J. Yin and C. He, *J. Am. Chem. Soc.*, 2010, **132**, 2567-9.
145. J. Liu, J. Karpus, S. V. Wegner, P. R. Chen and C. He, *J. Am. Chem. Soc.*, 2013, **135**, 3144-3149.
146. M. S. Koay, B. M. Janssen and M. Merckx, *Dalton Trans.*, 2013, **42**, 3230-3232.
147. S. V. Wegner, F. Sun, N. Hernandez and C. He, *Chem. Commun. (Camb.)*, 2011, **47**, 2571-2573.
148. D. Y. Zhang, M. Azrad, W. Demark-Wahnefried, C. J. Frederickson, S. J. Lippard and R. J. Radford, *ACS Chem. Biol.*, 2015, DOI: 10.1021/cb500617c.